Molecular Microbiology (2015) 96(2), 293–305 ■
doi:10.1111/mmi.12936
First published online 12 February 2015

Histidine phosphocarrier protein regulates pyruvate kinase A activity in response to glucose in *Vibrio vulnificus*

Hey-Min Kim,[1] Young-Ha Park,[1] Chang-Kyu Yoon[1] and Yeong-Jae Seok[1,2]*

[1]*Department of Biological Sciences and Institute of Microbiology, Seoul National University, Seoul 151-742, South Korea.*

[2]*Department of Biophysics and Chemical Biology, Seoul National University, Seoul 151-742, South Korea.*

Summary

The bacterial phosphoenolpyruvate:sugar phosphotransferase system (PTS) consists of two general energy-coupling proteins [enzyme I and histidine phosphocarrier protein (HPr)] and several sugar-specific enzyme IIs. Although, in addition to the phosphorylation-coupled transport of sugars, various regulatory roles of PTS components have been identified in *Escherichia coli*, much less is known about the PTS in the opportunistic human pathogen *Vibrio vulnificus*. In this study, we have identified pyruvate kinase A (PykA) as a binding partner of HPr in *V. vulnificus*. The interaction between HPr and PykA was strictly dependent on the presence of inorganic phosphate, and only dephosphorylated HPr interacted with PykA. Experiments involving domain swapping between the PykAs of *V. vulnificus* and *E. coli* revealed the requirement for the C-terminal domain of *V. vulnificus* PykA for a specific interaction with *V. vulnificus* HPr. Dephosphorylated HPr decreased the K_m of PykA for phosphoenolpyruvate by approximately fourfold without affecting V_{max}. Taken together, these findings indicate that the *V. vulnificus* PTS catalyzing the first step of glycolysis stimulates the final step of glycolysis in the presence of glucose through the direct interaction of dephospho-HPr with the C-terminal domain of PykA.

Introduction

Vibrio vulnificus is a Gram-negative, curved rod-shaped marine bacterium with a single flagellum. This bacterium is an opportunistic human pathogen that causes serious and often fatal infections. These include an invasive septicemia usually contracted through the consumption of raw or undercooked shellfish, as well as wound infections acquired through contact with shellfish or marine waters where the organism is present (Strom and Paranjpye, 2000). Primary septicemia is the most lethal infection caused by *V. vulnificus*, with an average mortality rate exceeding 50%. The majority of septic patients die of fulminant septicemia within 48 h after infection. Risk factors for severe *V. vulnificus* infection include any chronic disease, liver disease, alcoholism and diabetes (Bross *et al.*, 2007).

The bacterial phosphoenolpyruvate (PEP):sugar phosphotransferase system (PTS) plays an important role in the translocation of numerous sugars across the cytoplasmic membrane. The PTS is composed of two general cytoplasmic proteins, enzyme I (EI) and histidine phosphocarrier protein (HPr), and a set of sugar-specific proteins collectively known as enzyme IIs (EIIs) (Postma *et al.*, 1993). For example, glucose-specific EII of *Escherichia coli* consists of soluble $EIIA^{Glc}$ and membrane-bound $EIICB^{Glc}$. EI and HPr mediate phosphoryl transfer from PEP to EII, which ultimately phosphorylates PTS sugar substrates during uptake. Therefore, the ratio of the phosphorylated forms of PTS components increases in the absence and decreases in the presence of a PTS sugar.

Components of the PTS also participate in numerous physiological processes. The regulatory roles of the PTS have been most extensively studied in *E. coli*, and these roles include regulation of chemotaxis by EI (Lux *et al.*, 1995), regulation of glycogen phosphorylase, the BglG antiterminator and the anti-σ^{70} factor Rsd by HPr (Amster-Choder and Wright, 1990; Seok *et al.*, 1997; 2001; Rothe *et al.*, 2012; Park *et al.*, 2013), and regulation of the global repressor Mlc by the membrane-bound glucose transporter $EIICB^{Glc}$ (Lee *et al.*, 2000; Tanaka *et al.*, 2000; Nam *et al.*, 2001; 2008). In addition, $EIIA^{Glc}$ regulates carbohydrate transport and metabolism (Hurley *et al.*, 1993; Postma *et al.*, 1993; Seok *et al.*, 1997), the metabolic flux between fermentation and respiration (Koo *et al.*, 2004), and adenylyl cyclase activity (Park *et al.*, 2006). These regulatory functions of the PTS depend on the phosphorylation state of the involved components.

Like the *E. coli* PTS, the two general components (EI and HPr) and $EIIA^{Glc}$ are encoded by the *ptsHIcrr* operon, and $EIICB^{Glc}$ is encoded separately by *ptsG* in *V. vulnifi-*

Accepted 14 January, 2015. *For correspondence. E-mail yjseok@snu.ac.kr; Tel. (+82) 2 880 8827; Fax (+82) 2 888 4911.

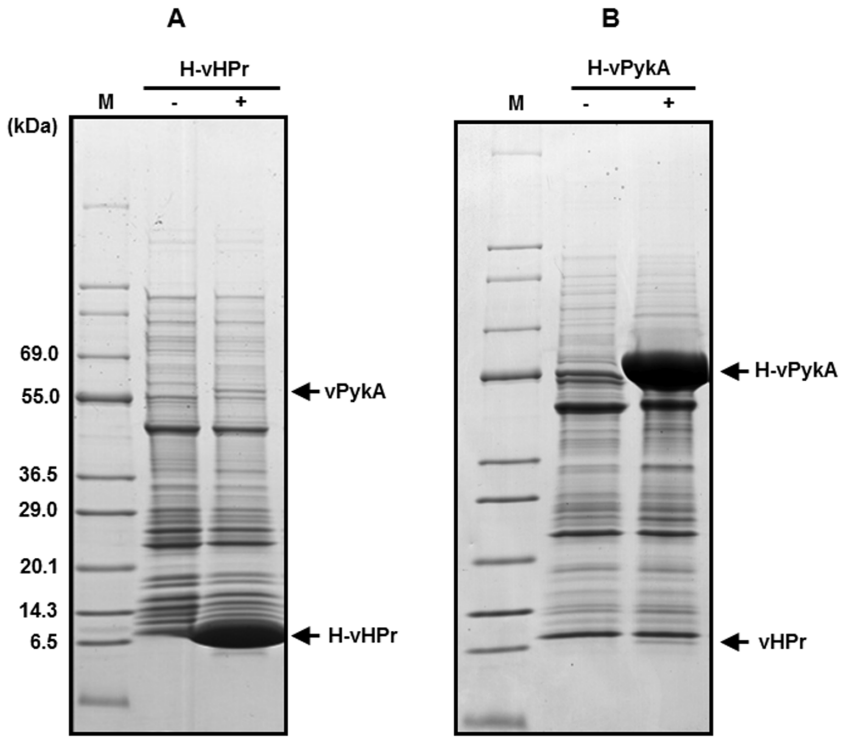

Fig. 1. Specific interaction of PykA with HPr in *V. vulnificus*. Ligand fishing experiments to search for protein(s) interacting with H-vHPr (A) and H-vPykA (B) were carried out as described in the *Experimental procedures*. Crude extract prepared from *V. vulnificus* CMCP6 cells was mixed with TALON metal affinity resin in the presence (lane +) or absence (lane –) of purified His-tagged protein bait and subjected to metal affinity chromatography. After a brief wash, proteins bound to the resin were eluted, and the eluates were analyzed by SDS-PAGE using 4–20% gradient gels followed by staining with Coomassie brilliant blue. The protein bands that specifically bound to H-vHPr and H-vPykA were excised from gels, and in-gel digestion and peptide mapping of tryptic digests were carried out as described previously (Jeong *et al.*, 2004). EzWay Protein Blue MW Marker (KOMA Biotech) was used as the molecular mass marker (lane M).

cus. However, much less is known about the regulatory roles of the *V. vulnificus* PTS. In *V. vulnificus*, $EIIA^{Glc}$ is known to regulate the activity of insulin degrading enzymes (Kim *et al.*, 2010) and the fermentation/respiration switch protein FrsA, which has been proposed as a cofactor-independent decarboxylase (Lee *et al.*, 2011).

To date, there has been no direct evidence for the participation of EI and HPr in the regulation of other metabolic pathways in *V. vulnificus*. *V. vulnificus* HPr is a small protein with an M_r of 9094 predicted based on its amino acid sequence. Given that HPr is known to be more abundant than $EIIA^{Glc}$ in enteric bacteria (Rohwer *et al.*, 2000), we assumed that there might be some regulatory mechanisms associated with HPr.

In this study, a ligand-fishing strategy was employed to discover the high affinity binding of HPr to a protein from *V. vulnificus* extracts. The protein was purified and determined to be an ortholog of *E. coli* pyruvate kinase A (ePykA). Pyruvate kinase (PK) catalyzes the final step of glycolysis, which is the transfer of a phosphoryl group from PEP to ADP, generating the products ATP and pyruvate for anaerobic and aerobic metabolism (Munoz and Ponce, 2003; Zoraghi *et al.*, 2010). This reaction is essentially irreversible *in vivo* and appears to be one of the major control points for the regulation of glycolytic flux. In addition, both the substrates and products of this reaction feed into a number of energetic and biosynthetic pathways, placing PK at a crucial metabolic intersection. Here, we demonstrate that HPr is a phosphorylation state-dependent allosteric effector of the ePykA ortholog in *V. vulnificus*.

Results

Specific interaction between HPr and pyruvate kinase A in V. vulnificus

To search for a protein(s) that interacts with *V. vulnificus* HPr (hereafter vHPr), we used a ligand fishing strategy (Lee *et al.*, 2007; Kim *et al.*, 2010; 2011; Park *et al.*, 2013). *V. vulnificus* CMCP6 crude extract was mixed with an N-terminally His_6-tagged form of vHPr (H-vHPr) and subjected to a pull-down assay. In several repeated experiments, we identified a protein band migrating with an apparent molecular mass of approximately 52 kDa that always co-eluted with H-vHPr (Fig. 1A). Peptide mapping of this protein band employing MALDI-TOF mass spectrometry analysis following in-gel digestion with trypsin indicated that the protein corresponded to a provisional PK encoded by *VV1_2992*.

Because PK catalyzes the final step of glycolysis, it is widespread in almost all types of organisms including animals, plants, fungi and protists as well as bacteria. BLAST searches revealed that *V. vulnificus* strains have three genes encoding PK isozymes (*VV1_2992*, *VV1_0644* and *VV2_0206*) like other vibrios. In contrast, *E. coli* strains have two PK isozymes: PykA (ePykA) is

known to be allosterically activated by AMP, whereas PykF (ePykF) known to be allosterically activated by fructose 1,6-bisphosphate. The PK encoded by *VV1_0644* shares 78% and 38% amino acid sequence identity with ePykF and ePykA of the *E. coli* K-12 strain, respectively, whereas the protein encoded by *VV1_2992* demonstrates 37% and 71% identity with ePykF and ePykA respectively (Fig. S1A). Although the PK encoded by *VV2_0206* shares a slightly higher sequence identity with ePykA (52%) than ePykF (40%), the presence of few mRNA transcripts of *VV2_0206* observed when the *V. vulnificus* CMCP6 strain was cultivated in different growth media suggests that *VV2_0206* expression may be cryptic (Fig. S1B). Therefore, hereafter we refer to the PKs encoded by *VV1_0644* and *VV1_2992* as vPykF and vPykA respectively.

To confirm the interaction between vPykA and vHPr, we purified His_6-tagged vPykA. A pull-down assay was performed using TALON metal affinity resin (Takara Bio, Japan) charged with H-vPykA to identify vPykA-binding proteins from *V. vulnificus* CMCP6 crude extract. After a brief wash, proteins bound to the resin were eluted with 200 mM imidazole and analyzed by SDS-PAGE. As shown in Fig. 1B, a protein band migrating slightly slower than the 6.5 kDa polypeptide was detected only in the eluate from the column loaded with crude extract in the presence of H-vPykA. Peptide mass fingerprinting after in-gel tryptic digestion of this protein band revealed four peptides derived from vHPr with a sequence coverage of 65.9% (56/85 amino acids, data not shown). This result supports a specific interaction between vHPr and vPykA.

Dependence of the interaction between vHPr and vPykA on inorganic phosphate

To examine whether the interaction between vHPr and vPykA requires any additional factor(s), purified vPykA was mixed with purified H-vHPr and subjected to metal affinity chromatography. Unlike vPykA in crude cell extracts, the purified protein alone exhibited little binding to H-vHPr unless crude cell extract was added (Fig. 2A, lanes 1–3), implying that the interaction between vHPr and vPykA depends on an additional factor(s). To test whether this additional factor is a protein or a small metabolite, the crude cell extract was filtered using a Microsep 3K membrane (Pall/Gelman Laboratory), and the effect of the filtrate on the interaction was measured. Because vPykA exhibited binding to H-vHPr in the presence of the filtrate, we assumed that the factor required for the vPykA–vHPr interaction could be a small molecule (Fig. 2A, lane 4). Therefore, we tested the effects of various cellular metabolites on this interaction. Although potassium glutamate, potassium acetate and acetyl phosphate had little effect on vHPr-vPykA binding, potassium phosphate remarkably increased the binding of vPykA to vHPr (Fig. 2A, lanes 5–8), indicating that inorganic phosphate (P_i) is the mediator of the vHPr–vPykA interaction. It should be noted that 50 mM sodium phosphate buffer was used in the initial fishing experiment to search for a new binding partner of vHPr (Fig. 1).

Intracellular concentrations of P_i have been reported in the range of 3–9 mM for *E. coli* grown under normal conditions in the pioneering *in vivo* ^{31}P-NMR studies (Ugurbil *et al.*, 1982), although internal P_i can rise to higher levels when glycerol-3-phosphate is added to the medium (Xavier *et al.*, 1995). Therefore, we tested the effect of P_i concentration on the interaction between vHPr and vPykA. Consistent with the data in Fig. 2A, vPykA showed little specific binding to H-vHPr in the absence of P_i (Fig. 2B, lanes 1 and 2). However, as the concentration of P_i in the reaction mixtures was raised, the specific binding of vPykA to H-vHPr increased as well (Fig. 2B and C). A double reciprocal plot revealed that the P_i concentration for half-maximal stimulation of the vPykA–vHPr interaction was approximately 3.95 mM (Fig. 2D). Considering this result and the intracellular concentrations of P_i reported in *E. coli* (Ugurbil *et al.*, 1982), P_i was added to a final concentration of 10 mM, resulting in approximately 70% maximum stimulation, in all experiments hereafter unless otherwise specifically mentioned.

Phosphorylation state-dependent interaction between vHPr and vPykA

The specificity of the interaction between vHPr and vPykA was determined by employing surface plasmon resonance (SPR) biosensor technology with the BIAcore 3000 system (GE Healthcare) (Seok *et al.*, 1997). vHPr was immobilized on a CM5 sensor chip, and vPykA or vPykF was allowed to flow over the surface. When purified vPykF was exposed to immobilized vHPr, no interaction was detected (Fig. 3A, sensorgram a). In contrast, purified vPykA resulted in a significant increase in the SPR response (Fig. 3A, sensorgram b). Specificity of the interaction between vPykA and vHPr was also confirmed by pull-down assays using TALON metal affinity resin charged with purified H-vPykA or purified H-vPykF in the absence and presence of 10 mM P_i (Fig. S2A). When a fixed amount of purified vHPr was mixed with H-vPykA, the amount of vHPr pulled down by H-vPykA increased only in the presence of 10 mM P_i. However, H-vPykF adsorbed to TALON metal affinity resin did not pull down vHPr regardless of the presence of P_i, indicating that the inorganic phosphate-dependent interaction of vHPr is specific for vPykA and does not occur with vPykF.

To determine kinetic parameters for the binding of vHPr to vPykA, different concentrations (31.25–500 μM) of purified vPykA were applied to the vHPr surface of the sensor chip. The signal increased as a function of vPykA concen-

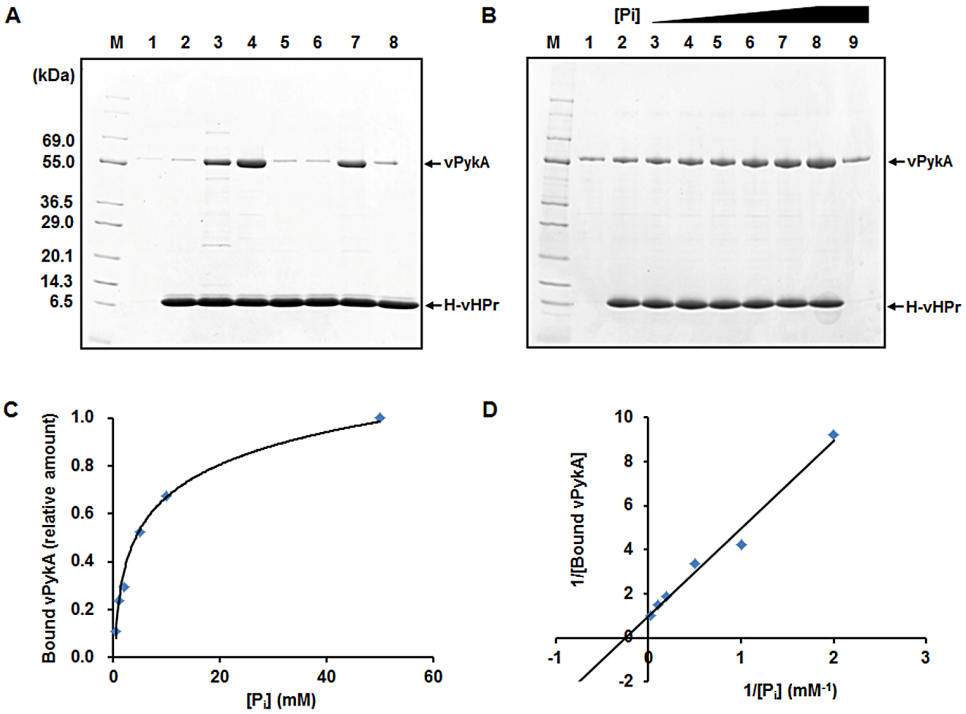

Fig. 2. The interaction between vPykA and vHPr depends on inorganic phosphate.
A. The effect of various compounds on the interaction of vPykA with vHPr. Purified vPykA (100 μg) was mixed with purified H-vHPr (60 μg) in 20 mM HEPES–NaOH (pH 7.6) containing 150 mM NaCl in the presence or absence of various compounds and subjected to TALON metal affinity chromatography. The results were analyzed by 4–20% gradient SDS-PAGE and staining with Coomassie brilliant blue. Lane M, molecular mass markers (KOMA Biotech); lane 1, vPykA was added alone as control; lane 2, vPykA and H-vHPr; lane 3, vPykA, H-vHPr and 50 μl of *V. vulnificus* crude extract used in Fig. 1; lane 4, vPykA, H-vHPr, 50 μl of 3-kDa filtrate of *V. vulnificus* crude extract; lane 5, vPykA, H-vHPr and potassium glutamate (to 10 mM); lane 6, vPykA, H-vHPr, potassium acetate (to 10 mM); lane 7, vPykA, H-vHPr, potassium phosphate (to 10 mM); lane 8, vPykA, H-vHPr and acetyl phosphate (to 10 mM).
B. Effect of varying concentrations of sodium phosphate (P_i) on the interaction of vPykA with vHPr. vPykA (100 μg) and H-vHPr (60 μg) in 20 mM HEPES–NaOH (pH 7.6) containing 150 mM NaCl were incubated with increasing amounts of P_i (0, 0.5, 1, 2, 5, 10 and 50 mM; lanes 2–8) and subjected to pull-down assays. In lanes 1 and 9, vPykA alone was incubated with 0 and 50 mM P_i, respectively, and subjected to pull-down assays as a loading control.
C. Plot of the P_i concentration-dependent binding of vPykA to H-vHPr. The Coomassie blue-stained gel in (B) was scanned, and the band intensities of vPykA were measured with the Multi Gauge program. The relative amounts of vPykA bound to H-vHPr were calculated based on the specific binding by subtracting the amount of vPykA bound to H-vHPr in 0 mM P_i from that bound to H-vHPr in each concentration of P_i as indicated.
D. Double reciprocal plot of 1/[Bound vPykA] *versus* 1/[P_i] using the data in (C).

tration (Fig. 3B). The dissociation constant (K_D) for the vHPr-vPykA interaction was determined using BIAevaluation software to be approximately 4.5×10^{-7} M, assuming a 1:1 interaction.

Generally, the regulatory functions of the PTS depend on the phosphorylation state of the involved protein (Deutscher *et al.*, 2006). Accordingly, the effect of phosphorylation of vHPr on its interaction with vPykA was assessed by SPR. The phosphorylated and dephosphorylated vHPr surfaces were generated by reversible phosphoryl transfer reactions between EI, vHPr and $EIIA^{Glc}$ (Nam *et al.*, 2001). When purified vPykA was applied to immobilized vHPr, a high affinity interaction was detected (Fig. 3C, sensorgram a). In contrast, after immobilized vHPr was phosphorylated by allowing the mixture of EI and PEP to flow over the surface and was subsequently washed with running buffer, an interaction with vPykA was barely detectable (Fig. 3C, sensorgram b). Furthermore, the same vHPr surface demonstrated recovered vPykA binding activity after dephosphorylation by flowing dephosphorylated $EIIA^{Glc}$ through the flow cell and flushing with running buffer (Fig. 3C, sensorgram c). These results indicate that only dephospho-vHPr, but not its phospho-form, can interact with vPykA.

Specificity and dependence on phosphorylation state for the interaction between vHPr and vPykA was also examined via pull-down assays with H-vHPr adsorbed to TALON metal affinity resin. The phosphorylated form of vHPr was generated by adding EI and PEP to the reaction mixtures (Fig. S3). As expected for enzymes requiring divalent cations as cofactors (Muirhead, 1990), some nonspecific binding of both vPykA and vPykF to TALON metal affinity resin was observed. When a fixed amount of purified vPykA was mixed with different concentrations of dephos-

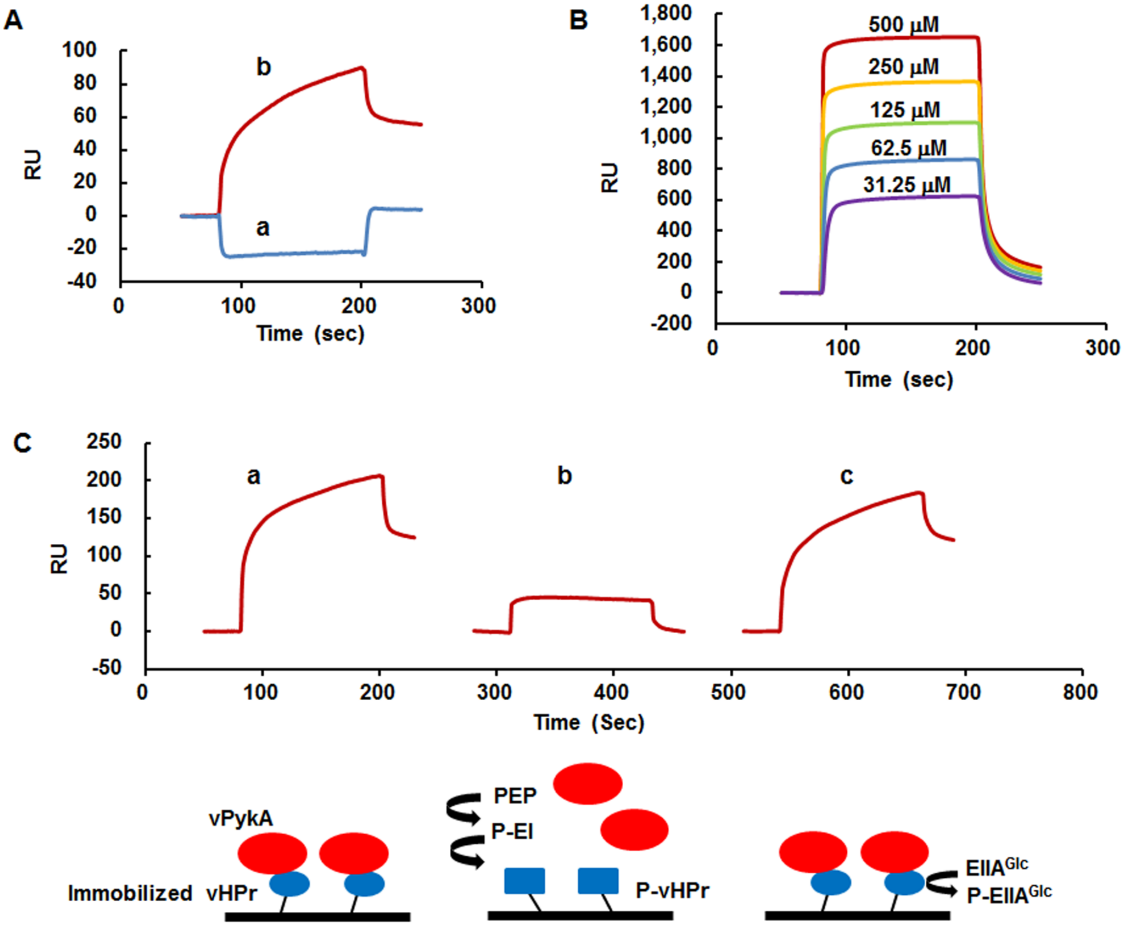

Fig. 3. Analysis of the interaction between vHPr and vPykA by surface plasmon resonance (SPR).
A. vPykF (sensorgram a) or vPykA (sensorgram b) was allowed to flow over the vHPr surface.
B. Measurement of the dissociation constant (K_D) between vPykA and vHPr. The indicated amounts of vPykA were allowed to flow over the vHPr surface. The K_D value for the interaction between vHPr and vPykA was determined to be ~4.484×10^{-7} M.
C. Phosphorylation state-dependent interaction between vPykA and vHPr. Sensorgram a shows vPykA binding to the immobilized vHPr surface. In sensorgram b, vPykA was injected after the immobilized vHPr surface had been phosphorylated by exposing it to a mixture of EI and phosphoenolpyruvate (PEP), then flushing with running buffer to remove PEP and EI. In sensorgram c, dephosphorylated $EIIA^{Glc}$ was allowed to flow over the phosphorylated vHPr surface generated in sensorgram b to dephosphorylate the surface before vPykA was injected.

phorylated H-vHPr, the amount of vPykA pulled down by H-vHPr increased as the concentration of H-vHPr increased (Fig. S2B). In contrast, when H-vHPr was phosphorylated by incubating with EI and PEP, the amount of vPykA bound to the resin was not affected by the concentration of vHPr added to the reaction mixture. As expected from the data in Fig. 3A, H-vHPr adsorbed to TALON metal affinity resin did not pull down vPykF regardless of the phosphorylation state of vHPr (Fig. S2C). These results support the specificity and dependence on the phosphorylation state of the vHPr–vPykA interaction.

The C-terminal domain of vPykA determines the binding specificity of the vHPr–vPykA complex

In a recent screen of proteins interacting with HPr employing a ligand fishing strategy in *E. coli*, we identified the anti-σ^{70} factor Rsd as a new target regulated by HPr (Park *et al.*, 2013). Whereas Rsd and glycogen phosphorylase, which has already been found to interact with HPr, were pulled down by HPr, we could not detect any interaction between HPr and PKs in *E. coli*. However, because BLAST searches revealed that vPykA and vHPr share 71% and 76% amino acid sequence identity with ePykA and *E. coli* HPr (hereafter eHPr), respectively, we assumed that the interaction of PykA with HPr might also occur in *E. coli*. To test whether the interaction between HPr and PykA is specific in *V. vulnificus* or whether cross-interactions are possible between proteins from other species, we prepared the HPr and PK proteins from *E. coli* and *V. vulnificus* and measured the cross-interactivities of these proteins. Notably, neither vHPr nor eHPr interacted with vPykF and ePykA, whereas vPykA did interact with eHPr, albeit with lower affinity than with vHPr (Fig. 4A). These

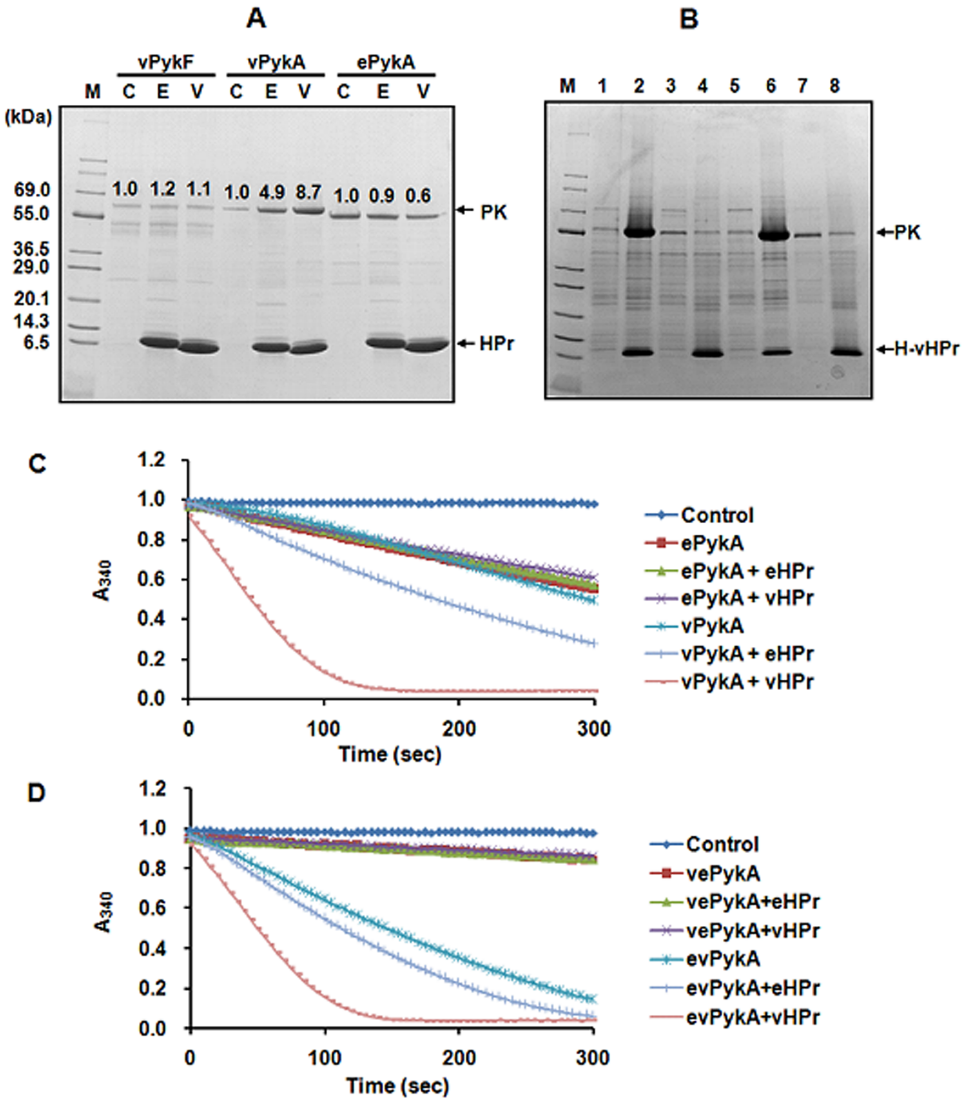

Fig. 4. Test for the interaction and allosteric effect between PKs and HPr proteins.
A. Purified vPykF, vPykA and ePykA (60 μg each) were mixed with buffer control (lane C), 100 μg of H-eHPr (lane E) or H-vHPr (lane V) in the presence of 50 μl of TALON resin. After metal affinity chromatography, proteins bound to each column were analyzed by 4–20% gradient SDS-PAGE and staining with Coomassie brilliant blue. Numbers above the PK bands represent the levels of PKs bound to HPr proteins relative to the level in lane C for each PK measured with Multi Gauge software. Lane M, molecular mass markers (KOMA Biotech).
B. After partial purification, vPykA (lanes 1 and 2), vePykA (lanes 3 and 4), evPykA (lanes 5 and 6) and ePykA (lanes 7 and 8) were subjected TALON affinity chromatography in the absence (odd-numbered lanes) and presence (even-numbered lanes) of H-vHPr. Lane M, molecular mass markers (KOMA Biotech).
C and D. The rates of PEP (1 mM) conversion to pyruvate catalyzed by four different PKs (native forms of ePykA and vPykA in (C) and two domain-swapped PKs in (D), 20 nM each) were measured by a lactate dehydrogenase (LDH)-coupled assay in the presence of 20 μM of eHPr or vHPr as indicated.

data indicate that the interaction between the HPr and PykA proteins is species-specific and dependent on the surface structure of PykA.

PKs are highly conserved in all organisms from prokaryotes to eukaryotes. The generation of crystal structures for several PKs from various species of bacteria, yeast and mammals has revealed a generally conserved architecture (Mattevi *et al.*, 1995; Rigden *et al.*, 1999; Valentini *et al.*, 2002; Zoraghi *et al.*, 2011). PKs exist as homo-tetramers, and each subunit consists of three or four domains: the N, A, B and C domains. The N domain is not present in prokaryotic PKs, and the A and B domains at N-termini of these bacterial enzymes comprise 70%, where binding sites for ADP, PEP and divalent cations are located. The remaining 30% corresponds to the C domain, where the binding site for the allosteric regulator is located. Alignment

of the amino acid sequences of ePykA and vPykA revealed that the 333 N-terminal amino acids are highly conserved with 78% identity, whereas the C-terminal domains are less conserved (Fig. S4A). Therefore, we assumed that the C-terminal domain of vPykA might determine binding specificity for vHPr. To explore the determinant of the species-specific interaction between PykA and HPr and verify our assumption, two chimeric PKs were constructed via a domain-swapping approach. The vePykA protein was made by fusing the N-terminal domain (amino acids 1–333) of vPykA to the C-terminal domain (amino acids 334–480) of ePykA, whereas the evPykA protein consisted of the N-terminal domain (amino acids 1–318) of ePykA and the C-terminal domain (amino acids 319–482) of vPykA. The sequences of all the constructs were confirmed by DNA sequencing. After partial purification, each chimeric PK was mixed with a fixed amount of H-vHPr and subjected to pull-down assays using TALON metal affinity resin. When vePykA and ePykA were mixed with H-vHPr, no interaction was detected (Fig. 4B, lanes 3, 4, 7 and 8). In contrast, when vPykA and evPykA were incubated with H-vHPr, they were pulled down by TALON resin (Fig. 4B, lanes 1, 2, 5 and 6). These results led us to conclude that the C-terminal domain of vPykA determines the binding specificity of the vHPr–vPykA complex.

The phosphorylation state of HPr is important for the regulation of vPykA activity

Because the binding site for the allosteric effector is located at the C-terminal domain of PKs (Larsen *et al.*, 1994; Jurica *et al.*, 1998) and the C-terminal domain determines the specificity of the HPr–PykA interaction, we tested whether HPr can act as an allosteric regulator of PykA. PK activity was determined by a lactate dehydrogenase (LDH)-coupled assay that measures the decrease in absorbance at 340 nm resulting from the oxidation of NADH to NAD^+. This assay is based on the conversion of PEP to pyruvate by PK, coupled to the conversion of pyruvate to lactate by LDH at the expense of NADH (Zoraghi *et al.*, 2010). To investigate whether the specific interaction of HPr and PykA is directly related to the specific regulation of PK activity, four different PKs (vPykA, evPykA, vePykA and ePykA) were purified (Fig. S4B), and their activities were compared in the presence and absence of eHPr or vHPr (Fig. 4C and D). vPykA demonstrated approximately the same specific activity as ePykA. However, the chimeric protein vePykA comprising an N-terminal two-thirds from vPykA linked to a C-terminal one-third from ePykA exhibited a significantly lower specific activity, whereas evPykA consisting of an N-terminal two-thirds from ePykA and a C-terminal one-third from vPykA showed a considerably higher specific activity than that of vPykA and ePykA. As expected from the binding assays (Fig. 4A), ePykA activity was little affected by either eHPr or vHPr, whereas vPykA activity was significantly stimulated by vHPr. eHPr also stimulated vPykA activity, albeit to a much lesser degree than vHPr (Fig. 4C). Notably, the enzyme activity of vePykA was not stimulated by either eHPr or vHPr, whereas evPykA behaved in a manner similar to vPykA in terms of activity regulation by vHPr and eHPr (Fig. 4D). These results are in accordance with the data from the binding assays (Fig. 4A and B) and indicate that HPr stimulates enzyme activity by binding to the allosteric site in the C-terminal domain of vPykA.

vPykA activity was determined in the presence of varying concentrations of AMP, fructose 1,6-bisphosphate (FBP) and dephosphorylated vHPr (Fig. 5). As expected given its high sequence identity with ePykA (71%) and low sequence identity with ePykF (37%), vPykA activity was not significantly influenced by FBP. Interestingly, however, vPykA was activated by 8 mM AMP by only approximately twofold, whereas ePykA was activated more than 10-fold (Fig. 5A). Dephospho-vHPr increased vPykA activity in a concentration-dependent manner up to approximately sevenfold compared with the level in control assays (Fig. 5B). From these data, it can be assumed that the *in vivo* allosteric effector of vPykA might be dephospho-vHPr rather than AMP. The stimulation of vPykA activity by dephospho-vHPr was saturable, with maximal activation at 16 μM of vHPr and half-maximal activation at approximately 4 μM.

We also investigated the effect of the phosphorylation state of vHPr on the regulation of vPykA activity. To determine if phosphorylation of vHPr would affect its stimulatory activity, PEP (1 mM), EI (4 μg ml^{-1}) and variable concentrations of vHPr were added to a coupled enzyme assay. This reaction mixture was preincubated for 5 min before the assay was initiated by the addition of vPykA, as we confirmed that vHPr could be completely phosphorylated under this condition (Fig. S3, last lane). Notably, the addition of phospho-vHPr resulted in no stimulation of vPykA activity regardless of the amount of vHPr, indicating that only dephospho-vHPr can interact with and thus stimulate the activity of vPykA.

To evaluate the effect of vHPr on the catalytic function of vPykA, steady-state kinetics of vPykA were determined with respect to PEP in the absence and presence of 20 μM dephospho-vHPr (Fig. 5C). Parameters derived from these kinetics are summarized in Table 1. Although vHPr showed little, if any, effect on the V_{max}, Hill coefficient (h) and catalytic activity (k_{cat}) of vPykA, the presence of vHPr led to an approximately 3.7-fold decrease in the $S_{0.5}$ of PEP under nonsaturation conditions. These data imply that the phosphorylation state of vHPr regulates vPykA activity by influencing the affinity of vPykA for PEP.

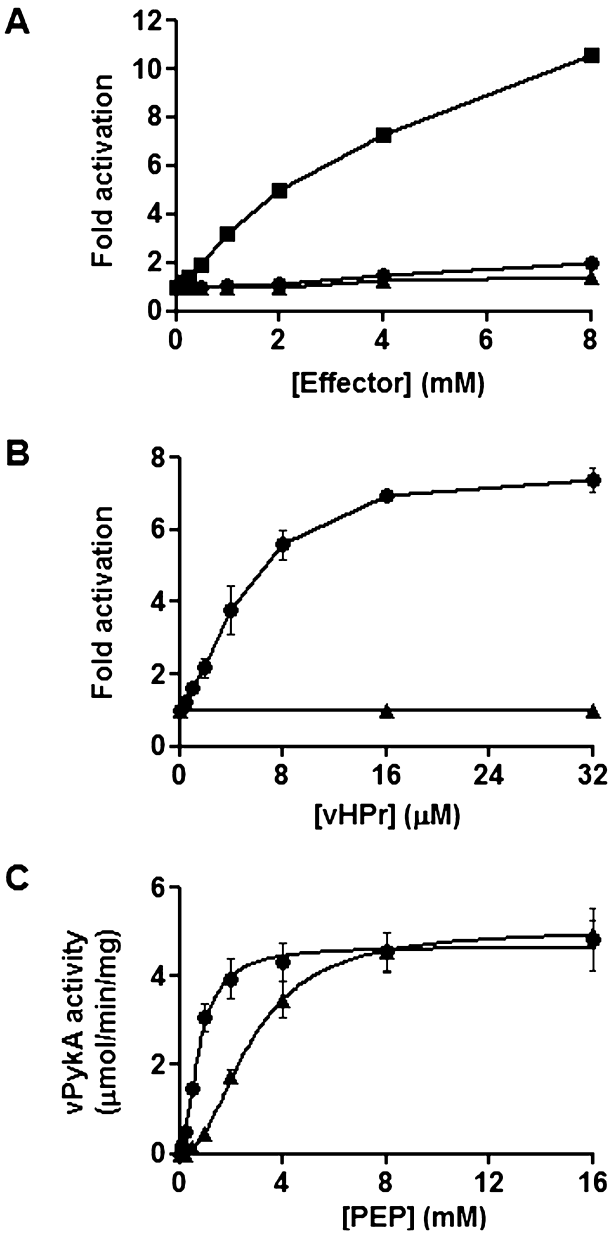

Fig. 5. The allosteric regulation of vPykA.
A. Effects of varying concentrations of AMP (0–8 mM) on ePykA (squares) and vPykA (circles) activity. The effects of various concentrations of fructose 1,6-bisphosphate (0–8 mM) on vPykA (triangles) were also measured.
B. The effects of varying amounts of dephospho-vHPr (circles) and phospho-vHPr (triangles) on vPykA activity. The results are presented as the mean ± standard deviations ($n = 3$).
C. Steady-state kinetics of vPykA were determined with respect to PEP (0–16 mM) in the absence (triangles) and presence (circles) of 20 μM dephospho-vHPr. vPykA and ePykA were added to 20 nM. The results are presented as the mean ± standard deviations ($n = 3$). The resultant kinetic parameters are presented in Table 1.

The in vivo *phosphorylation state of vHPr and its effect on vPykA activity are dependent on the presence of glucose*

It is generally accepted that the phosphorylation states of the PTS components vary according to the availability of PTS substrates and the metabolic state of the cell (Deutscher *et al.*, 2014). Indeed, it has recently been revealed that eHPr is almost completely dephosphorylated in Luria-Bertani (LB) medium supplemented with the PTS sugar glucose, whereas it exists mainly in the phosphorylated form in LB medium supplemented with a non-PTS sugar in *E. coli* (Park *et al.*, 2013). To determine whether the phosphorylation state of vHPr also depends on the availability of a PTS sugar, we measured the phosphorylation level of vHPr in cells grown in LB medium containing 2.5% NaCl (LBS) supplemented with either glucose or galactose. As shown in Fig. S5, vHPr was mostly dephosphorylated in LBS medium supplemented with glucose, whereas it was predominantly in the phosphorylated state in LBS medium and LBS medium supplemented with galactose (a non-PTS sugar in *V. vulnificus*). Therefore, it could be assumed that vHPr regulates vPykA activity in response to the availability of a preferred PTS sugar, which determines the phosphorylation state of vHPr.

To confirm the phosphorylation state-dependent effect of vHPr on vPykA activity *in vivo*, we measured the intracellular concentrations of PEP and pyruvate in wild-type CMCP6 and *pykA* mutant cells grown on glucose or galactose after the addition of respective carbon sources. In the wild-type strain, the pyruvate concentration drastically increased with a concomitant decrease in the PEP concentration within 5 min after the addition of 10 mM glucose (Fig. 6A and B). Notably, the pyruvate concentration also increased in *pykA* deletion mutant cells after the addition of glucose, but to a considerably lesser extent than in wild-type cells, with a slight decrease in the PEP concentration. In the *pykA* mutant strain transformed with the plasmid pRK-PKA in which vPykA expression is under the control of its own promoter, the pyruvate concentration increased to a level similar to (or slightly higher than) that of the wild-type strain, with only a slight decrease in the PEP level after the addition of 10 mM glucose. However, the addition of the non-PTS sugar galactose did not cause

Table 1. Kinetic parameters of vPykA with respect to PEP in the presence and absence of vHPr.

	–vHPr	+vHPr
V_{max} (μmol min^{-1} mg^{-1})	5.04 ± 0.14	4.66 ± 0.14
h	2.16 ± 0.18	1.86 ± 0.23
$S_{0.5}$ (mM)	2.74 ± 0.14	0.74 ± 0.06
k_{cat} (sec^{-1})	4.31 ± 0.12	3.98 ± 0.12

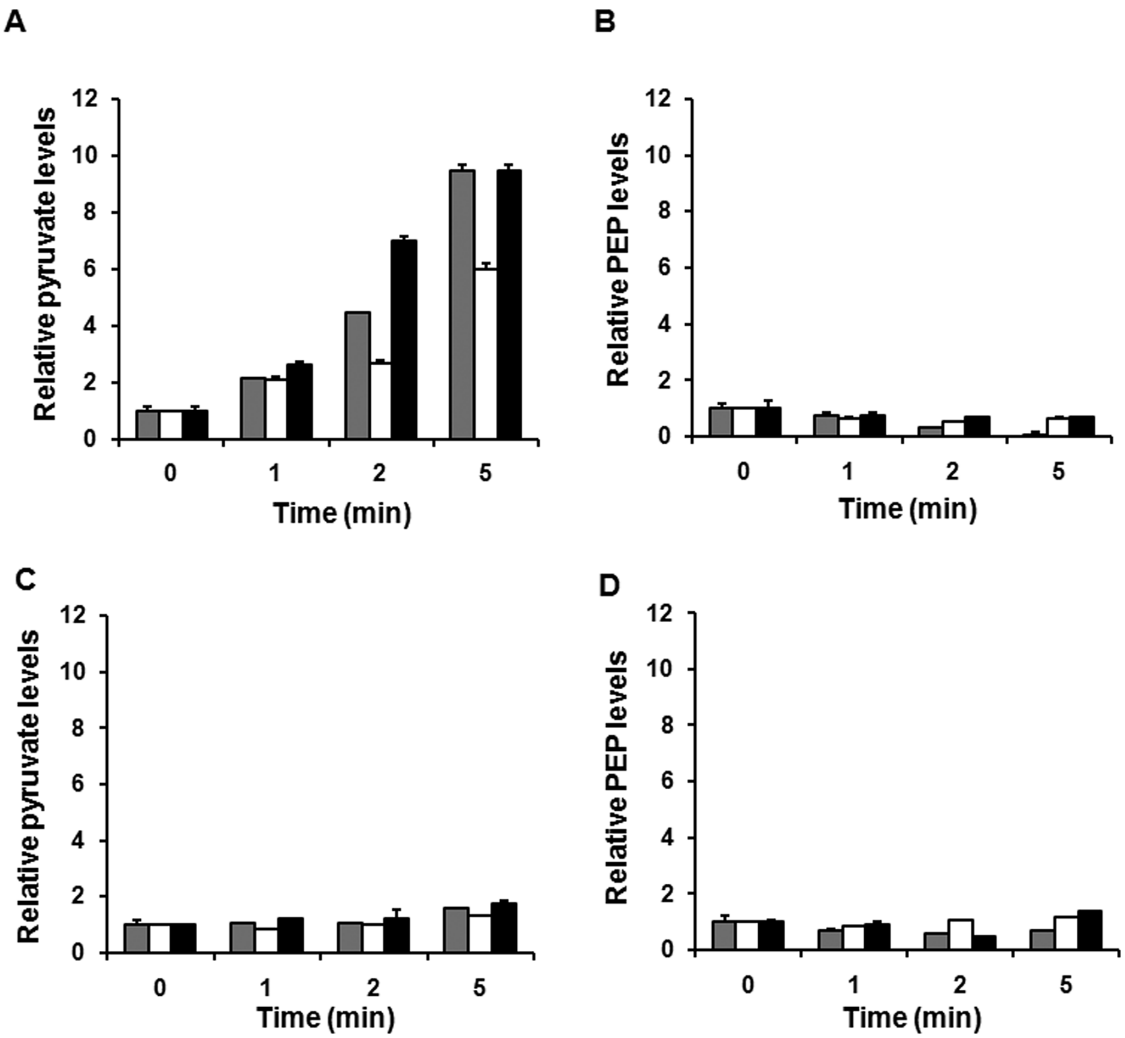

Fig. 6. Changes in the intracellular concentrations of PEP and pyruvate after the addition of glucose or galactose.
A–D. The intracellular concentrations of pyruvate (A and C) and PEP (B and D) were measured as described in the *Experimental procedures*. Samples were prepared from wild-type CMCP6 (gray bars), the *pykA* deletion mutant (white bars) and the *pykA* deletion mutant harboring a vPykA expression vector (black bars) at the indicated time points after the addition of 10 mM glucose (A and B) or galactose (C and D). The results are presented as the mean ± standard deviations ($n = 3$).

any remarkable changes in the intracellular concentrations of pyruvate and PEP in all three strains (Fig. 6C and D). It should be noted that the significant difference in the pyruvate concentrations depending on the carbon source was not due to the differential effects of the two sugars on *pykA* expression in *V. vulnificus* (Fig. S1C). Therefore, our data suggest that vPykA plays, at least in part, a role in the regulation of the cellular levels of pyruvate by interacting with dephospho-vHPr, which increases in the presence of PTS substrates.

Discussion

Because dephosphorylated forms of the PTS components increase during transport of a preferred PTS substrate such as glucose, the PTS also functions as a sensory system for monitoring environmental changes such as nutrient availability. In this study, we provide evidence that the general PTS component HPr stimulates activity of the pyruvate kinase PykA in response to the availability of glucose in the opportunistic human pathogen *V. vulnificus*. Regulation of the glycolytic flux by an HPr homolog through direct protein–protein interaction is also known in *Bacillus subtilis*. It was previously shown that only the dephosphorylated form of Crh, the paralog of HPr, interacted with methylglyoxal synthase MgsA in *B. subtilis* (Landmann *et al.*, 2011). This interaction inhibited the enzyme activity of MgsA and thus decreased the conversion of dihydroxyacetone-phosphate to highly cytotoxic methylglyoxal. Methylglyoxal can be further metabolized

to lactate and pyruvate, representing an energetically unfavorable bypass of glycolysis. Therefore, the regulation of the glycolytic flux by HPr or its homologous proteins through phosphorylation state-dependent protein–protein interaction is likely to be widespread among bacteria.

The PTS catalyzes the first step of glycolysis, which is the coupled transport and phosphorylation of sugars, whereas PK catalyzes the final step of glycolysis, specifically the irreversible conversion of PEP to pyruvate with concomitant phosphorylation of ADP to ATP. The maximal stimulation of vPykA activity by dephospho-vHPr could be obtained at approximately 16 μM of vHPr up to sevenfold compared with the level in control assays without the addition of vHPr (Fig. 5B). The intracellular concentration of HPr was previously calculated to be 20–100 μM in *E. coli* and *Salmonella typhimurium* (Mattoo and Waygood, 1983; Rohwer *et al.*, 2000). Similar to eHPr in *E. coli* cells (Park *et al.*, 2013), vHPr exists mainly in the phosphorylated form in LBS medium and LBS medium supplemented with galactose, which is a non-PTS sugar, whereas it is predominantly found in the dephosphorylated state in medium supplemented with glucose, which is a PTS sugar in *V. vulnificus* cells (Fig. S5). These data suggest that the concentration of dephosphorylated HPr can vary from 0 to 100 μM, and the total activity of vPykA can change up to sevenfold in cells depending on the carbon source. Because this regulation does not occur in *E. coli*, it thus seems likely that the regulatory roles of the PTS reflect species-specific metabolic needs.

It is quite interesting that the regulatory interactions of HPr with its target proteins are species-specific. Despite the fact that both *E. coli* and *V. vulnificus* belong to γ-proteobacteria, and thus orthologous proteins in the two species share high amino acid sequence identity (33% for Rsd, 47% for glycogen phosphorylase, 71% for PykA and 76% for HPr), we could not detect either Rsd or glycogen phosphorylase from *V. vulnificus* extracts in repeated ligand fishing experiments using vHPr as bait. Although ePykA cannot bind to either eHPr or vHPr, eHPr binds to vPykA and stimulates its activity, albeit to a much lesser degree than does vHPr. Because phosphorylation at His 15 of vHPr abolishes its interaction with vPykA, it could be assumed that the binding surface on vHPr would include amino acid residues near His 15. Comparison of the amino acid sequence of eHPr with that of vHPr indicates that amino acid residues located near His 15 on the three-dimensional structure of eHPr are quite well conserved, except for Pro11 and Glu85 (Glu 11 and His85 in vHPr respectively) (Fig. S6). Therefore, the difference in these two residues might, at least in part, explain the lower affinity of eHPr to vPykA. Structural studies on the vHPr–vPykA complex will help to understand the species-specific nature of this regulatory interaction between vHPr and vPykA.

It is also interesting that the specific PK activities of the two PykA proteins from *E. coli* and *V. vulnificus* change reciprocally after swapping the C-domain, where the binding site for the allosteric effector is located. It was previously shown that the allosteric transition between the inactive T-state and the active R-state involved a symmetrical 6° rigid-body rocking motion of the A- and C-domain cores in each of the four subunits to alter tetramer rigidity (Morgan *et al.*, 2010). Therefore, the reciprocal changes in the specific PK activities of the two PykA proteins after the C-domain swap might be attributable to changes in tetramer rigidity. Structural studies of these hybrid proteins are required to fully understand the mechanisms underlying of this reciprocal activity swap.

Although no direct interaction has yet been demonstrated between PKs and the PTS, the possibility for interaction between them has previously been raised in firmicutes. Analysis of the numerous available genome sequences has revealed that firmicutes possess a PK with a C-terminal extension that strongly resembles the phosphorylation domain of EI (Nguyen and Saier, 1995). Even though the phosphorylatable histidine is conserved, attempts to phosphorylate the EI domain of the PK with PEP or PEP plus EI and HPr have not been successful (Deutscher *et al.*, 2006). Nevertheless, the presence of this EI-like sequence suggests that PKs might interact with HPr in firmicutes.

Experimental procedures

Bacterial strains, plasmids and culture conditions

The bacterial strains and plasmids used in this study are listed in Table S1. *V. vulnificus* strains were cultured in Luria-Bertani medium containing 2.5% NaCl (LBS) or M9 minimal medium containing 0.2% casamino acids and 2.5% NaCl (M9S). All *E. coli* strains were grown in LB medium.

To construct a *pykA* deletion mutant of the *V. vulnificus* CMCP6 strain, a 1079 bp DNA containing the *pykA* upstream region was amplified from the genomic DNA of *V. vulnificus* CMCP6 using two primers; 5′-GACCGTCTCGAGGCAC CCTCTGTTGCCACAG-3′ (synthetic XhoI site underlined) and 5′-TGGCTGTCTAGAAGCTTCTCCTGCGATAGAC-3′ (synthetic XbaI site underlined). The polymerase chain reaction (PCR) product was then cloned into the pDM4 vector (Milton *et al.*, 1996) to produce pDM-PKAup. An 881 bp DNA fragment containing the downstream region of the *pykA* gene was amplified using the primers 5′-GTTTTTTCTAGACTC GCTTCATTAGTGATAG-3′ (synthetic XbaI site underlined) and 5′-AAAATTAGATCTTATCCCTATAAGTTGGATC-3′ (synthetic BglII site underlined) and cloned into the corresponding sites of pDM-PKAup to result in pDM-ΔPKA. The *E. coli* SM10 λ*pir* strain carrying pDM-ΔPKA was conjugated with *V. vulnificus* CMCP6, and the transconjugants were selected, and integration was confirmed by PCR. To generate a *pykA* deletion mutant, the exoconjugants were then selected in LBS containing 8% sucrose (Lee *et al.*, 2011). Deletion of *pykA* in the selected colonies was confirmed by PCR.

To construct pRK-PKA, an 1,879-bp DNA fragment containing the *V. vulnificus pykA* gene and its own promoter was amplified using two primers, 5′-CATCTTGGATCCCAACA TTCTATAACGGAGC-3′ (engineered BamHI site underlined) and 5′-CCAGTTCTGCAGTCAGCGGCCGAGACGAATTG-3′ (engineered PstI site underlined). The PCR product was cloned into the broad-host-range plasmid pRK415. The resultant plasmid, pRK-PKA, was transformed into *E. coli* SM10 λ*pir*, and then transferred to the *pykA* mutant of *V. vulnificus* by conjugation.

All plasmids were constructed using standard PCR-based cloning techniques and verified by sequencing (see Table S1).

Construction of chimeric PykA proteins

To construct pET-vePykA, a 998-bp DNA fragment containing the *V. vulnificus pykA* gene was amplified from the genomic DNA of *V. vulnificus* CMCP6 using two primers, 5′-AG GAGAACATATGACTCAGCCATTAAGAAG-3′ (engineered NdeI site underlined) and 5′-ACTTCTGCCATGGAGCGC ACCGTTTCGACTGG-3′ (engineered NcoI site underlined). The PCR product was then cloned into the pET3a vector to produce pET-vPykAup. A 445-bp DNA fragment containing the *E. coli pykA* gene was amplified from the genomic DNA of *E. coli* MG1655 using the primers 5′-TTGCAGCCATGGCGC GCGTTTGCCTGGGTGC-3′ (engineered NcoI site underlined) and 5′-CCGGCAGGATCCTTACTCTACCGTTAAAAT ACG-3′ (engineered BamHI site underlined) and cloned into the corresponding sites of pET-vPykAup to result in pET-vePykA.

To construct pET-evPykA, an 840-bp DNA fragment containing the *E. coli pykA* gene was amplified from the genomic DNA of *E. coli* MG1655 using two primers, 5′-AGTATTCCAT GGGCTCCAGAAGGCTTCGCAGAAC-3′ (primer A, engineered NcoI site underlined) and 5′-GTGTTGCCGTGATTAC CGCTCGGTTTAGCTGAC-3′. A 609-bp DNA fragment containing the *V. vulnificus pykA* gene was amplified from the genomic DNA of *V. vulnificus* CMCP6 using the primers 5′-CTAAACCGAGCGGTAATCACGGCAACACAAATG-3′ and 5′-TAATGAGGATCCTTAGTCAAAAACAGGCAGG-3′ (primer B, engineered BamHI site underlined). The two PCR products were fused in a second round PCR using primers A and B, and the obtained fragment was cloned into the NcoI and BamHI sites of pETDuet-1 to produce pET-evPykA.

Protein purification

Proteins with N-terminal His tags used in this study were overexpressed in the *E. coli* BL21 (DE3) strain, and purified using TALON metal affinity resin (Takara Bio) according to the manufacturer's instructions. The proteins were eluted with 200 mM imidazole and further purified by gel filtration chromatography using a HiLoad 16/60 Superdex 75 prep grade column (GE Healthcare) in 20 mM HEPES–NaOH (pH 7.6) containing 150 mM NaCl. Untagged proteins were overexpressed in *E. coli* BL21 (DE3) (vPykA, vPykF, ePykA, evPykA, vePykA and vHPr) or the *E. coli* GI698*Δpts* strain (Nosworthy *et al.*, 1998) (eEI and eHPr). BL21 (DE3) cells were harvested 4 h after induction with 1 mM IPTG, and GI698*Δpts* cells were harvested 20 h after induction with 100 μg ml^{-1} tryptophan. Cells were then disrupted by passing twice through a French pressure cell at 10 000 psi and were centrifuged at 100 000 *g* for 30 min at 4°C. The proteins in the supernatants were then purified using Mono Q 10/100 and HiLoad 16/60 Superdex 75 prep grade (GE Healthcare) column chromatography. Protein concentrations were determined with a bicinchoninic acid protein assay (Pierce) or Bradford assay (Bio-Rad).

Ligand fishing to search for proteins interacting with vHPr

V. vulnificus CMCP6 cells grown at 30°C overnight in LBS (100 ml) were harvested, washed and resuspended in 3 ml of buffer A (50 mM sodium phosphate, pH 7.0, containing 150 mM NaCl). Cells were disrupted by passing twice through a French pressure cell at 10 000 psi and then centrifuged at 100 000 *g* for 30 min at 4°C. The supernatant (1 ml) was mixed with 0.5 mg of His-tagged protein bait, and this mixture was incubated with 100 μl of TALON metal affinity resin at 4°C for 30 min. After incubation, the resin was harvested and washed with 1 ml of buffer A three times, and the proteins bound to the resin were eluted with 100 μl of 2 × SDS sample buffer. Aliquots of the eluted protein samples were analyzed by SDS-PAGE and staining with Coomassie brilliant blue.

RNA isolation and quantitative reverse transcription PCR (qRT-PCR)

Total RNA was prepared using an RNeasy Mini kit (Qiagen) from *V. vulnificus* CMCP6 cells grown to logarithmic phase in LBS and M9S medium containing 0.2% glucose or galactose, and qRT-PCR was performed as described previously (Park *et al.*, 2013). DNA was removed using an RNase-free DNase (Promega).

Surface plasmon resonance spectroscopy

The real-time interaction of vHPr with vPykA or vPykF was monitored by SPR detection using a BIAcore 3000 (BIAcore AB) as described previously (Lee *et al.*, 2007; Park *et al.*, 2013). Purified vHPr was immobilized on the carboxymethylated dextran surface of a CM5 sensor chip using a NHS/EDC reaction. The standard running buffer was 10 mM potassium phosphate (pH 7.5), 150 mM NaCl, 10 mM KCl, 1 mM $MgCl_2$ and 1 mM dithiothreitol (DTT), and all reagents were introduced at a flow rate of 10 μl min^{-1}. The K_D value was determined using BIAevaluation 2.1 software.

Measurement of PK activity

Pyruvate kinase activity was determined by a continuous assay coupled to LDH, in which the change in absorbance at 340 nm due to oxidation of NADH was measured using a spectrophotometer. The reaction contained 100 mM HEPES–NAOH (pH 7.5), 200 mM KCl, 10 mM $MgCl_2$, 10 mM sodium phosphate, 1 mM DTT, 0.2 mM NADH, and 6 units of LDH

(Sigma-Aldrich) in a total volume of 1 ml. Two millimolar ADP and 0–16 mM PEP were added as substrates to determine $S_{0.5}$ of vPykA for PEP in the presence or absence of 20 μM dephospho-vHPr. Reactions were initiated by the addition of vPykA to a total concentration of 20 nM and continued at 30°C for 5 min. PK activity was expressed as specific activity (μmol min^{-1} mg^{-1}), which is defined as the amount of PK that catalyzes the formation of 1 μmol of pyruvate per min. The apparent $S_{0.5}$, Hill coefficient (*h*), and V_{max} or k_{cat} values were determined by allosteric sigmoidal nonlinear regression analysis of data using the Prism software package (Graph Pad Inc., San Diego, CA, USA).

Determination of the intracellular PEP and pyruvate concentrations

To determine the intracellular concentrations of PEP and pyruvate, 800 ml of cells were grown to A_{600} = 1, harvested by centrifugation and washed with ice-cold M9S without a carbon source. Cells were diluted to a final volume of 2.6 ml with M9S, adjusted to room temperature for 5 min and aerated for 2 min before the indicated carbon source was added. Aeration was continued throughout the experiment. Samples (500 μl) were taken at the indicated times, mixed immediately with 250 μl of 5 M $HClO_4$, vortexed for 5 s and centrifuged at 5000 *g* for 20 min at 4°C. Supernatants (500 μl) were neutralized with 170 μl of 5 M K_2CO_3. Precipitated $KClO_4$ was removed by centrifugation for 5 min in a chilled Eppendorf centrifuge. PEP and pyruvate were analyzed using spectrophotometry (Hogema *et al.*, 1998). The reaction mixture (total 1 ml) contained 200 μl of each sample plus 500 μl of reaction buffer containing 200 mM HEPES-NaOH (pH 7.5), 20 mM $MgCl_2$, 400 mM KCl, 2 mM DTT and 10 μl of freshly prepared 20 mM NADH. To measure pyruvate, the reaction was started by the addition of 1.5 units of LDH (Sigma-Aldrich). The A_{340} was observed after incubating at 30°C for 20 min. Subsequently, for the determination of PEP, a PK (1 unit)/LDH (1.4 units) mixture (Sigma-Aldrich) was added with ADP (to 2 mM), and the A_{340} was observed after incubating at 30°C for 20 min.

Acknowledgements

This work was supported by National Research Foundation Grants NRF 2010-0017384 funded by the Ministry of Science, ICT, and Future Planning, Republic of Korea. HMK was supported by the Fellowship for Fundamental Academic Fields from Seoul National University.

Author contributions

H.M.K., Y.H.P. and Y.J.S. designed the study and analyzed the data; H.M.K., Y.H.P. and C.K.Y. performed the experiments; and H.M.K., Y.H.P. and Y.J.S. wrote the paper.

Conflict of interest

The authors declare that they have no conflict of interest.

References

Amster-Choder, O., and Wright, A. (1990) Regulation of activity of a transcriptional anti-terminator in *E. coli* by phosphorylation in vivo. *Science* **249:** 540–542.

Bross, M.H., Soch, K., Morales, R., and Mitchell, R.B. (2007) *Vibrio vulnificus* infection: diagnosis and treatment. *Am Fam Physician* **76:** 539–544.

Deutscher, J., Francke, C., and Postma, P.W. (2006) How phosphotransferase system-related protein phosphorylation regulates carbohydrate metabolism in bacteria. *Microbiol Mol Biol Rev* **70:** 939–1031.

Deutscher, J., Ake, F.M., Derkaoui, M., Zebre, A.C., Cao, T.N., Bouraoui, H., *et al.* (2014) The bacterial phosphoenolpyruvate:carbohydrate phosphotransferase system: regulation by protein phosphorylation and phosphorylation-dependent protein-protein interactions. *Microbiol Mol Biol Rev* **78:** 231–256.

Hogema, B.M., Arents, J.C., Bader, R., Eijkemans, K., Yoshida, H., Takahashi, H., *et al.* (1998) Inducer exclusion in *Escherichia coli* by non-PTS substrates: the role of the PEP to pyruvate ratio in determining the phosphorylation state of enzyme IIA^{Glc}. *Mol Microbiol* **30:** 487–498.

Hurley, J.H., Faber, H.R., Worthylake, D., Meadow, N.D., Roseman, S., Pettigrew, D.W., and Remington, S.J. (1993) Structure of the regulatory complex of *Escherichia coli* III^{Glc} with glycerol kinase. *Science* **259:** 673–677.

Jeong, J.Y., Kim, Y.J., Cho, N., Shin, D., Nam, T.W., Ryu, S., and Seok, Y.J. (2004) Expression of *ptsG* encoding the major glucose transporter is regulated by ArcA in *Escherichia coli*. *J Biol Chem* **279:** 38513–38518.

Jurica, M.S., Mesecar, A., Heath, P.J., Shi, W., Nowak, T., and Stoddard, B.L. (1998) The allosteric regulation of pyruvate kinase by fructose-1,6-bisphosphate. *Structure* **6:** 195–210.

Kim, H.J., Lee, C.R., Kim, M., Peterkofsky, A., and Seok, Y.J. (2011) Dephosphorylated NPr of the nitrogen PTS regulates lipid A biosynthesis by direct interaction with LpxD. *Biochem Biophys Res Commun* **409:** 556–561.

Kim, Y.J., Ryu, Y., Koo, B.M., Lee, N.Y., Chun, S.J., Park, S.J., *et al.* (2010) A mammalian insulysin homolog is regulated by enzyme IIA^{Glc} of the glucose transport system in *Vibrio vulnificus*. *FEBS Lett* **584:** 4537–4544.

Koo, B.M., Yoon, M.J., Lee, C.R., Nam, T.W., Choe, Y.J., Jaffe, H., *et al.* (2004) A novel fermentation/respiration switch protein regulated by enzyme IIA^{Glc} in *Escherichia coli*. *J Biol Chem* **279:** 31613–31621.

Landmann, J.J., Busse, R.A., Latz, J.H., Singh, K.D., Stulke, J., and Gorke, B. (2011) Crh, the paralogue of the phosphocarrier protein HPr, controls the methylglyoxal bypass of glycolysis in *Bacillus subtilis*. *Mol Microbiol* **82:** 770–787.

Larsen, T.M., Laughlin, L.T., Holden, H.M., Rayment, I., and Reed, G.H. (1994) Structure of rabbit muscle pyruvate kinase complexed with Mn^{2+}, K^+, and pyruvate. *Biochemistry* **33:** 6301–6309.

Lee, C.R., Cho, S.H., Yoon, M.J., Peterkofsky, A., and Seok, Y.J. (2007) *Escherichia coli* enzyme IIA^{Ntr} regulates the K^+ transporter TrkA. *Proc Natl Acad Sci USA* **104:** 4124–4129.

Lee, K.J., Jeong, C.S., An, Y.J., Lee, H.J., Park, S.J., Seok, Y.J., *et al.* (2011) FrsA functions as a cofactor-independent decarboxylase to control metabolic flux. *Nat Chem Biol* **7:** 434–436.

Lee, S.J., Boos, W., Bouche, J.P., and Plumbridge, J. (2000) Signal transduction between a membrane-bound transporter, PtsG, and a soluble transcription factor, Mlc, of *Escherichia coli*. *EMBO J* **19:** 5353–5361.

Lux, R., Jahreis, K., Bettenbrock, K., Parkinson, J.S., and Lengeler, J.W. (1995) Coupling the phosphotransferase system and the methyl-accepting chemotaxis protein-dependent chemotaxis signaling pathways of *Escherichia coli*. *Proc Natl Acad Sci USA* **92:** 11583–11587.

Mattevi, A., Valentini, G., Rizzi, M., Speranza, M.L., Bolognesi, M., and Coda, A. (1995) Crystal structure of *Escherichia coli* pyruvate kinase type I: molecular basis of the allosteric transition. *Structure* **3:** 729–741.

Mattoo, R.L., and Waygood, E.B. (1983) Determination of the levels of HPr and enzyme I of the phosphoenolpyruvate-sugar phosphotransferase system in *Escherichia coli* and *Salmonella typhimurium*. *Can J Biochem Cell Biol* **61:** 29–37.

Milton, D.L., O'Toole, R., Hörstedt, P., and Wolf-Watz, H. (1996) Flagellin A is essential for the virulence of *Vibrio anguillarum*. *J Bacteriol* **178:** 1310–1319.

Morgan, H.P., McNae, I.W., Nowicki, M.W., Hannaert, V., Michels, P.A., Fothergill-Gilmore, L.A., and Walkinshaw, M.D. (2010) Allosteric mechanism of pyruvate kinase from *Leishmania mexicana* uses a rock and lock model. *J Biol Chem* **285:** 12892–12898.

Muirhead, H. (1990) Isoenzymes of pyruvate kinase. *Biochem Soc Trans* **18:** 193–196.

Munoz, M.E., and Ponce, E. (2003) Pyruvate kinase: current status of regulatory and functional properties. *Comp Biochem Physiol B Biochem Mol Biol* **135:** 197–218.

Nam, T.W., Cho, S.H., Shin, D., Kim, J.H., Jeong, J.Y., Lee, J.H., *et al*. (2001) The *Escherichia coli* glucose transporter enzyme $IICB^{Glc}$ recruits the global repressor Mlc. *EMBO J* **20:** 491–498.

Nam, T.W., Jung, H.I., An, Y.J., Park, Y.H., Lee, S.H., Seok, Y.J., and Cha, S.S. (2008) Analyses of Mlc-IIB^{Glc} interaction and a plausible molecular mechanism of Mlc inactivation by membrane sequestration. *Proc Natl Acad Sci USA* **105:** 3751–3756.

Nguyen, C.C., and Saier, M.H., Jr (1995) Phylogenetic analysis of the putative phosphorylation domain in the pyruvate kinase of *Bacillus stearothermophilus*. *Res Microbiol* **146:** 713–719.

Nosworthy, N.J., Peterkofsky, A., Konig, S., Seok, Y.J., Szczepanowski, R.H., and Ginsburg, A. (1998) Phosphorylation destabilizes the amino-terminal domain of enzyme I of the *Escherichia coli* phosphoenolpyruvate:sugar phosphotransferase system. *Biochemistry* **37:** 6718–6726.

Park, Y.H., Lee, B.R., Seok, Y.J., and Peterkofsky, A. (2006) *In vitro* reconstitution of catabolite repression in *Escherichia coli*. *J Biol Chem* **281:** 6448–6454.

Park, Y.H., Lee, C.R., Choe, M., and Seok, Y.J. (2013) HPr antagonizes the anti-sigma70 activity of Rsd in *Escherichia coli*. *Proc Natl Acad Sci USA* **110:** 21142–21147.

Postma, P.W., Lengeler, J.W., and Jacobson, G.R. (1993) Phosphoenolpyruvate:carbohydrate phosphotransferase systems of bacteria. *Microbiol Rev* **57:** 543–594.

Rigden, D.J., Phillips, S.E., Michels, P.A., and Fothergill-Gilmore, L.A. (1999) The structure of pyruvate kinase from *Leishmania mexicana* reveals details of the allosteric transition and unusual effector specificity. *J Mol Biol* **291:** 615–635.

Rohwer, J.M., Meadow, N.D., Roseman, S., Westerhoff, H.V., and Postma, P.W. (2000) Understanding glucose transport by the bacterial phosphoenolpyruvate:glycose phosphotransferase system on the basis of kinetic measurements *in vitro*. *J Biol Chem* **275:** 34909–34921.

Rothe, F.M., Bahr, T., Stulke, J., Rak, B., and Gorke, B. (2012) Activation of *Escherichia coli* antiterminator BglG requires its phosphorylation. *Proc Natl Acad Sci USA* **109:** 15906–15911.

Seok, Y.J., Sondej, M., Badawi, P., Lewis, M.S., Briggs, M.C., Jaffe, H., and Peterkofsky, A. (1997) High affinity binding and allosteric regulation of *Escherichia coli* glycogen phosphorylase by the histidine phosphocarrier protein, HPr. *J Biol Chem* **272:** 26511–26521.

Seok, Y.J., Koo, B.M., Sondej, M., and Peterkofsky, A. (2001) Regulation of *E. coli* glycogen phosphorylase activity by HPr. *J Mol Microbiol Biotechnol* **3:** 385–393.

Strom, M.S., and Paranjpye, R.N. (2000) Epidemiology and pathogenesis of *Vibrio vulnificus*. *Microbes Infect* **2:** 177–188.

Tanaka, Y., Kimata, K., and Aiba, H. (2000) A novel regulatory role of glucose transporter of *Escherichia coli*: membrane sequestration of a global repressor Mlc. *EMBO J* **19:** 5344–5352.

Ugurbil, K., Rottenberg, H., Glynn, P., and Shulman, R.G. (1982) Phosphorus-31 nuclear magnetic resonance studies of bioenergetics in wild-type and adenosinetriphosphatase (1-) *Escherichia coli* cells. *Biochemistry* **21:** 1068–1075.

Valentini, G., Chiarelli, L.R., Fortin, R., Dolzan, M., Galizzi, A., Abraham, D.J., *et al*. (2002) Structure and function of human erythrocyte pyruvate kinase. Molecular basis of nonspherocytic hemolytic anemia. *J Biol Chem* **277:** 23807–23814.

Xavier, K.B., Kossmann, M., Santos, H., and Boos, W. (1995) Kinetic analysis by in vivo ^{31}P nuclear magnetic resonance of internal P_i during the uptake of *sn*-glycerol-3-phosphate by the *pho* regulon-dependent Ugp system and the *glp* regulon-dependent GlpT system. *J Bacteriol* **177:** 699–704.

Zoraghi, R., See, R.H., Gong, H., Lian, T., Swayze, R., Finlay, B.B., *et al*. (2010) Functional analysis, overexpression, and kinetic characterization of pyruvate kinase from methicillin-resistant *Staphylococcus aureus*. *Biochemistry* **49:** 7733–7747.

Zoraghi, R., Worrall, L., See, R.H., Strangman, W., Popplewell, W.L., Gong, H., *et al*. (2011) Methicillin-resistant *Staphylococcus aureus* (MRSA) pyruvate kinase as a target for bis-indole alkaloids with antibacterial activities. *J Biol Chem* **286:** 44716–44725.

Supporting information

Additional supporting information may be found in the online version of this article at the publisher's web-site.